



Karbala International Journal of Modern Science

Volume 8 | Issue 4

Article 1

Evaluating Accuracy of Solar Ground Station System Data

Emad Jaleel Mahdi

Ministry of Science and Technology, Renewable Energy Directorate, Baghdad

Ali K. Resen

Ministry of Science and Technology, Renewable Energy Directorate, Baghdad

Ahmed B. Khamees

Ministry of Science and Technology, Renewable Energy Directorate, Baghdad,

Mudar Ahmed Abdulsattar

Department of Pharmacy, Al-Rasheed University College, mudarahmed3@yahoo.com

Follow this and additional works at: <https://kijoms.uokerbala.edu.iq/home>



Part of the [Physics Commons](#)

Recommended Citation

Mahdi, Emad Jaleel; Resen, Ali K.; Khamees, Ahmed B.; and Abdulsattar, Mudar Ahmed (2022) "Evaluating Accuracy of Solar Ground Station System Data," *Karbala International Journal of Modern Science*: Vol. 8 : Iss. 4 , Article 1.

Available at: <https://doi.org/10.33640/2405-609X.3258>

This Research Paper is brought to you for free and open access by Karbala International Journal of Modern Science. It has been accepted for inclusion in Karbala International Journal of Modern Science by an authorized editor of Karbala International Journal of Modern Science. For more information, please contact abdulateef1962@gmail.com.



Evaluating Accuracy of Solar Ground Station System Data

Abstract

The solar radiation data is crucial for many solar applications. In this regard, this manuscript analyzed and compared the correctness of ground station data with data from the PVGIS. Empirical equations were adopted to build software. This software calculates the global, direct, diffuse, and rates of solar radiation data on two axes. The result of the analysis was employed to assess the compatibility, dependability, and confidence of these types of data. The comparison showed that vastly variations in some curves from dawn to sunset. In sum, every site exhibit variation in solar radiation station rates. These results could serve as a starting point for users of solar data when analyzing the expected uncertainty for a given data

Keywords

Solar radiation; Empirical equations software; Pyranometer; Ground station.

Creative Commons License



This work is licensed under a [Creative Commons Attribution-Noncommercial-No Derivative Works 4.0 License](https://creativecommons.org/licenses/by-nc-nd/4.0/).

RESEARCH PAPER

Evaluating Accuracy of Solar Ground Station System Data

Emad J. Mahdi ^a, Ali K. Resen ^a, Ahmed B. Khamees ^a, Mudar A. Abdulsattar ^{a,b,*}

^a Ministry of Science and Technology, Renewable Energy Directorate, Baghdad, Iraq

^b Department of Pharmacy, Al-Rasheed University College, Baghdad, Iraq

Abstract

The solar radiation data is crucial for many solar applications. In this regard, this manuscript analyzed and compared the correctness of ground station data with data from the PVGIS. Empirical equations were adopted to build software. This software calculates the global, direct, diffuse, and rates of solar radiation data on two axes. The result of the analysis was employed to assess the compatibility, dependability, and confidence of these types of data. The comparison showed that vastly variations in some curves from dawn to sunset. In sum, every site exhibit variation in solar radiation station rates. These results could serve as a starting point for users of solar data when analyzing the expected uncertainty for a given data.

Keywords: Solar radiation, Empirical equations software, Pyranometer, Ground station

1. Introduction

Solar systems usually contain a receiving surface that collects solar radiation, such as photovoltaic systems or solar collectors [1], to determine the optimal orientation of this surface. Therefore, it is possible to estimate the amount of solar energy collected by surfaces of different orientations. Actually, collecting energy has many difficulties. The incident angle of sunlight during the day varies continuously. The sunlight rarely encounters a stationary surface directly because different components of radiation (direct, scattered, and reflected on the earth) reach the surface from different angles [2,3]. According to the variation of climatic conditions, the availability of these various ingredients varies, too [4,5].

The hourly horizontal plane data must be transformed into tilt plane surface radiation data to perform an accurate mathematical framework [6]. The software consists of a set of equations based on solar equation data used to simulate sizing the solar thermal or photovoltaic systems professionally [7].

The radiation formulas and mathematical models are very profitable for understanding the important factors that affect rooftop solar collectors [8,9]. Measurements in the horizontal plane are usually the first step in determining solar radiation on inclined surfaces. Solar radiation is generally measured by two main types of instruments, pyrheliometers, and pyranometers [10]. The pyrheliometer measures the solar radiation as a direct beam with a small part of the radiation from the sky around the sun's disk. Generally, sunlight passes through a glass window toward the thermocouple (a device that converts heat into electricity) [11]. The generated electrical signal can be recorded and converted into W/m^2 . The pyrheliometer window acts as a filter that allows sunlight to pass only in the (0.3–3.0) μm range. A pyranometer is a device that measures total solar radiation (including scattered and direct) coming from a planetarium in a horizontal plane. This means that the device must give an unbiased response to radiation from all directions. It consists of a thermal sensor that is horizontally oriented and a glass dome that limits the

Received 10 February 2022; revised 14 August 2022; accepted 17 August 2022.
Available online 10 November 2022

* Corresponding author at:

E-mail addresses: Emad.jaleel@yahoo.com (E.J. Mahdi), alialbadry80@gmail.com (A.K. Resen), ahmedbader63@yahoo.com (A.B. Khamees), mudarahmed3@yahoo.com (M.A. Abdulsattar).

<https://doi.org/10.33640/2405-609X.3258>

2405-609X/© 2022 University of Kerbala. This is an open access article under the CC-BY-NC-ND license (<http://creativecommons.org/licenses/by-nc-nd/4.0/>).

wavelength range. The glass dome keeps viewing at 180° and protects the thermal sensor from air convection. A radiometry system is a set of techniques for measuring electromagnetic radiation. A radiometer is a device used for measuring different types of electromagnetic radiation.

For instance, the International Organization for Standardization (ISO) and the World Meteorological Organization (WMO) regulate the pyr heliometer measuring parameters.

The pyr heliometer must mount on top of a device that tracks the sun's path because it only 'sees' the solar disk.

Pyranometer is a sensor that transforms the solar energy received into an electrical signal processed by other computerized devices. It measures a specific section of the solar spectrum. Pyranometer is concerned with the cosine angle of solar radiation. The energy received perpendicular to the sensor (i.e., at 0° from the zenith refers to 1000 W/m² [12,13].

Broadband solar irradiance is commonly measured with radiometers. Radiometers are fitted with thermal detectors, because of their relatively consistent spectral sensitivity, across the complete solar radiation spectrum. A number of variables can alter the measurements. These variables include changes in temperature (the equipment is positioned outdoors where the temperature can range from (−20 to 70) C°. Other variables like wind, rain, and snow affect the measurements, too [14,15]. The measurement of the diffuse and global radiation incident on a horizontal surface is usually done by agencies such as the National Weather Service (NWS). For this purpose, the measurement network uses multiple sources of information. These sources include numerical weather models, ground measurements, and satellite imagery [16]. Numerical Weather Prediction (NWP) models are built on dynamic equations that predict atmospheric changes for several days that differ from initial conditions [17]. All other models are based on the numerical weather prediction (NWP) model, which is global and covers the entire earth. The model equations and inputs are determined on a three-dimensional grid extending perpendicular to the earth's surface. This is because the global models are computationally intensive. To dispose of high-quality ground measured series for the proposed solar resource assessment study. An analysis of solar data is needed to dispose of the correct time series of three types of radiations; They are Direct Normal Irradiance (DNI), Diffuse Horizontal Irradiance (DHI), and Global Horizontal Irradiance (GHI) [18,19].

Best practices must follow two levels of quality for reliable, accurate, and completeness of solar radiation measurements [20]:

A - Quality Control: Preparation towards data collection during measurement and transmission process.

B - Quality Analysis: Quality assessment assurance and enhancement. Quality analysis procedures established by the Baseline Surface Radiation Network (BSRN) and Atmospheric Radiation Measurement Program (ARM) from Pacific Northwest National Laboratory (PNNL) for ground-measured radiometric data will be applied.

These analyses will be carried out to identify and correct measurement errors. A report with the main incidents and data registered curves will be provided to the customer, allowing corrective control actions. A good performance of the station during the measurement campaign is essential to obtain the correct information on the solar radiation behavior throughout the year [21].

Geostationary Earth-orbiting (GEO) and Low-Earth-orbiting (LEO) satellites have two distinct orbits. Geostationary satellites are those that orbit above the equator at a constant altitude of around 36,000 km and are hence referred to as geostationary satellites. Satellites in low earth orbit small satellites in low Earth orbit circle around the earth in a circular path, collecting data as the planet rotates on its axis. To put it another way, in one 24-h period, an orbiting satellite can "see" the whole world twice. At 36,000 km altitude, GEO satellites appear to be stationary above the equator because their orbital period equals the earth's rotation. A geostationary satellite's field of view is fixed, so it sees the same area day and night. This is great for observing cloud patterns with visible and infrared radiometers. The constant viewing angles with the high temporal resolution are hallmarks of geostationary images. Generation (Meteosat-7), Meteosat Second Generation (MSG), Multifunctional Transport Satellites (MTSAT), and Geostationary Satellite Server (GOES), as well as atmospheric data from terra and aqua polar (LEO) satellites [22,23]. The main advantages of the use of images from GEO satellites are the following [24]:

- The GEO satellite simultaneously sees large areas of terrain, allowing it to know the spatial distribution of the information, as well as determine the relative differences between one zone to the other.

- When the information available (satellite images) belongs to the same area, it is possible to study the evolution of the values in one pixel of the image or a specific geographic zone.
- It is possible to know past situations when there are satellite images recorded and stored previously.

Geostationary Earth-Orbiting satellites can give a temporal resolution of up to 15 min and spatial resolution of up to one kilometer. Satellites take photos over broad areas and at high time resolution, allowing cloud identification and forecasting [25,26]. Further processing of this data yields a forecast for the spatial variability of solar radiation data at ground level. Hourly satellite-derived irradiation is more accurate than ground-based measurements for sites more than 25 km from a ground station. As a result, combining data from satellites and ground stations to estimate the earth's solar radiation could be a realistic option for maintaining a well-functioning electric grid [27,28].

All those who rely on data of the greatest quality can do so with a certain degree of assurance. If data quality is high, users will be able to generate more effective results. Accuracy of data is crucial because erroneous data leads to inaccurate conclusions. If the expected outcomes are incorrect, time, money, and resources are wasted. Accurate data increases the confidence required to make better decisions, improves production, efficiency, and marketing, and reduces expenses. Researchers want precise or reliable study processes so that study results are applicable and significant. For all reasons mentioned above, this study emphasized studying the validity of the data of solar ground stations used in more than one site.

In order to rely on these data, the accuracy of the ground measurement data must be compared with high accuracy data such as empirical programming equations and validated with satellite data. Furthermore, to obtain conformity behavior from the sunrise to sunset data. This will give reliable, accurate data to be adopted in the analysis of solar applications.

2. Experimental work

A research methodology was developed to compare the data of these ground stations for measuring solar radiation accuracy by building a Software program that uses the relationship of the empirical equation to calculate the rates of solar radiation mathematically. The software program was written in the programming language using the

visual basic net language. This software program calculates the different values of solar radiation (global, direct, and diffuse) and rates of solar radiation in two axes and all values related to the sun, such as solar angles, daylight hours, and air mass. This software program depends on the mechanism of work for calculating solar radiation rates on the entry of information sites such as latitude, longitude, and altitude above sea level, the standard longitude of the local time zone, the solar constant, the tilt angles of surface, the date of the day and the number of the month in the year. The amount of the solar constant where its value is $1367 \text{ (W/m}^2\text{)}$. In addition to comparing the data of these ground stations with high-accuracy satellite data, the PV-GIS website data was approved for its accuracy and reliability. The four days of the seasonal solstice in the year (3/21, 6/21, 9/21, and 12/12) were adopted to compare the data for these days. The solar radiation data from ground stations in (W/m^2) units were distributed on five sites distributed on the Iraqi map, which have the latitude and longitude:

- Site 1: $(32^\circ 19' \text{N}, 47^\circ .28' \text{E})$
- Site 2: $(31^\circ .58' \text{N}, 46^\circ .33' \text{E})$
- Site 3: $(32^\circ .41' \text{N}, 43^\circ .54' \text{E})$
- Site 4: $(31^\circ .57' \text{N}, 44^\circ .46' \text{E})$, and
- Site 5: $(31^\circ .4' \text{N}, 44^\circ 18' \text{E})$.

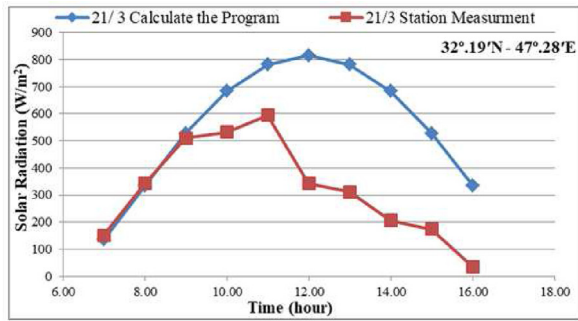
3. Results and discussion

This discussion is devoted to the results and discussion of the ground station data and comparison with other solar radiation data. And then explain the match the ground stations with the software program calculations and satellite data. In our work, solar radiation data were collected and typeset from five ground stations to measure solar radiation, which is distributed in several locations on the Iraqi map, according to the following latitude and longitude:

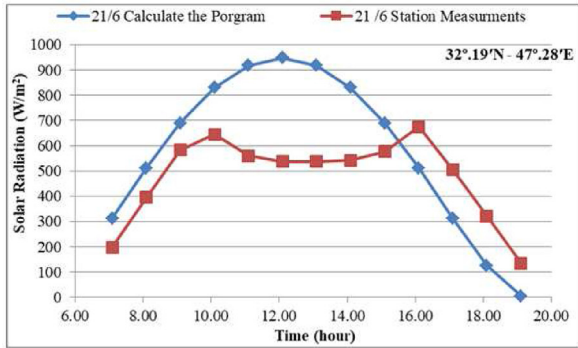
- Site 1: $(32^\circ 19' \text{N}, 47^\circ .28' \text{E})$
- Site 2: $(31^\circ .58' \text{N}, 46^\circ .33' \text{E})$
- Site 3: $(32^\circ .41' \text{N}, 43^\circ .54' \text{E})$
- Site 4: $(31^\circ .57' \text{N}, 44^\circ .46' \text{E})$, and
- Site 5: $(31^\circ .4' \text{N}, 44^\circ 18' \text{E})$.

In order to compare the accuracy of the solar radiation rates data for these stations, the four days of the seasonal solstice were adopted in the year (21/3, 21/6, 21/9, 21/12).

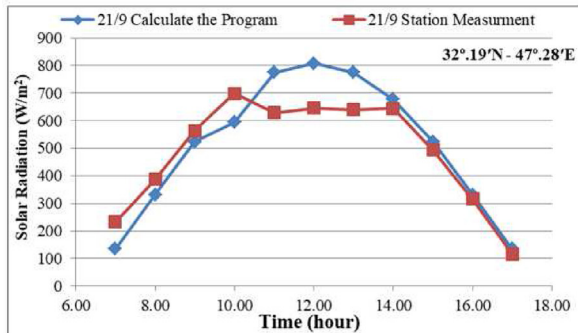
For the first site, we can notice from Fig. 1a that there is a correlation between the two types of data, but a clear contradiction occurs in the data of the



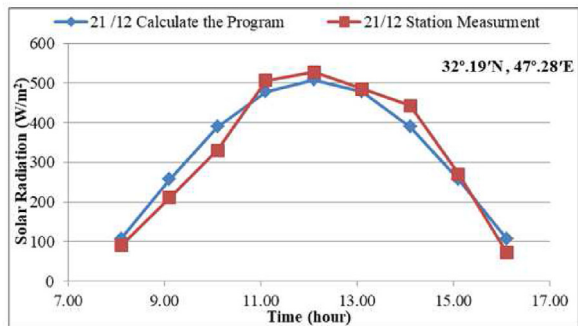
(a)



(b)



(c)



(d)

Fig. 1. Comparison between the measured and calculated data of solar radiation with time for site 1, in (a) 21/3, (b) 21/6, (c) 21/9, and (d) 21/12.

ground station at 10 o'clock, and the reason may be attributed to the weather conditions that the measurement station was exposed to, including clouds activity. Both curves continue to decrease until

sunset. In Fig. 1b, the two curves indicate the behaviour of the two types of data, which clearly indicates a shifting between two curves, and the shape of the curve represents the ground station data, where the curve takes a concavity pattern starting from 11 o'clock until 16 o'clock. The behavior of this curve indicates the effect of the sensor on weather factors, including attenuation to the solar radiation beam. In this ground station, there is some perfect alignment between the base level sensor with the base station.

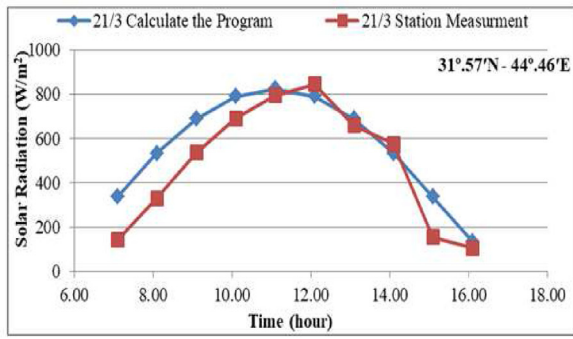
This shifting in Fig. 1b is clearly between the two curves when the altitude angle of the sun and the incidence angle of solar radiation change from one month to another, and the base level of the sensor are tilted towards the west.

In Fig. 1c, the two curves appear identical from the beginning of recording the solar radiation data until the middle of the day, as the ground station data curve begins to move away from the other curve and takes a different pattern and is recorded to measure the solar radiation less than the other curve, starting from 11 o'clock until 15 o'clock as attenuation to solar radiation, maybe by clouds activity. Fig. 1d represents a good fit for both curves. The curves show the same behavior as hourly solar radiation rates from sunrise to sunset.

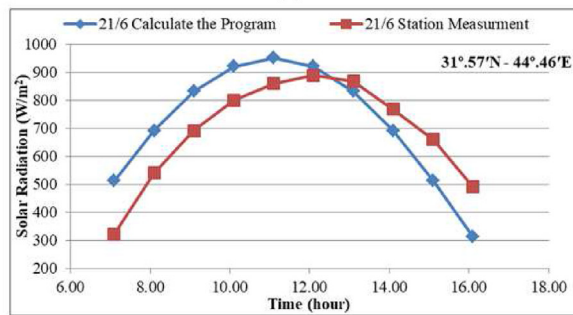
The results of the first site showed that the ground station was affected at times by installation factors, and this caused a shift in the curves of the ground data measurements. This shift between the two curves appears in Fig. 1c, and this shift will change the determination of the time of sunrise and sunset, as well as the time of the peak at midday; as for the other figures, it appears between the two curves that one of them is behaving outward and the second inward, and this determines the field of view of the solar sensor. But it seems that the matter is different in site 2; it can be seen clearly that both curves behave the same and that there is a good match between them, except in Fig. 2b, d, there is a little shift at the peak of the curve to ground station measurements and may be attributed to the base level of the sensor and status of ground station installing respectively. This indicates that the reliability and accuracy of this station's data are very good.

Fig. 2 shows the comparison between ground station measurements and calculations of the program in time periods for site 2.

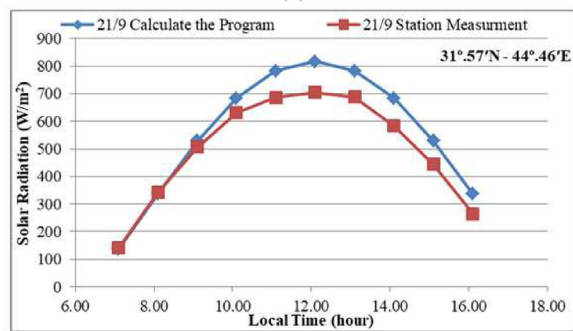
In site 2, the shift between the two curves appears for more than a month, and there is a tendency for this shift toward the west; this shift does not specify midday with high accuracy because the installation process for the station was not accurate in this site.



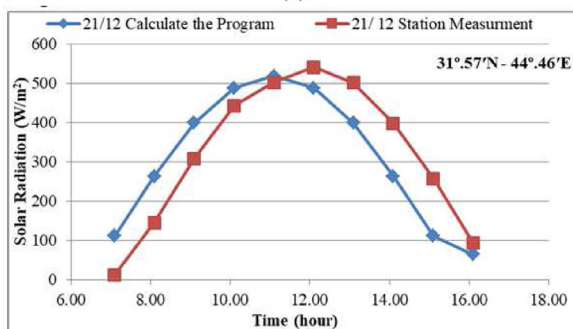
(a)



(b)

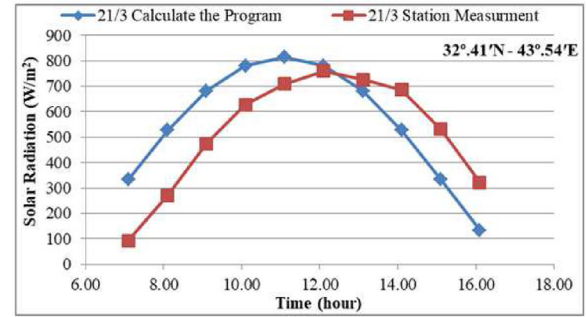


(c)

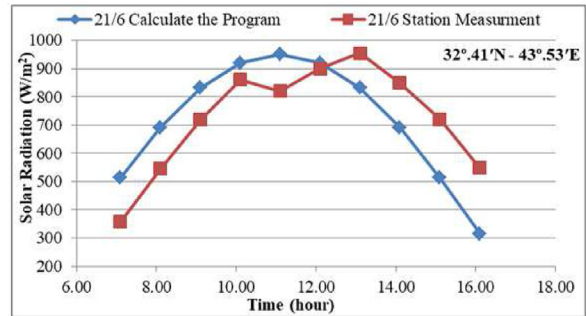


(d)

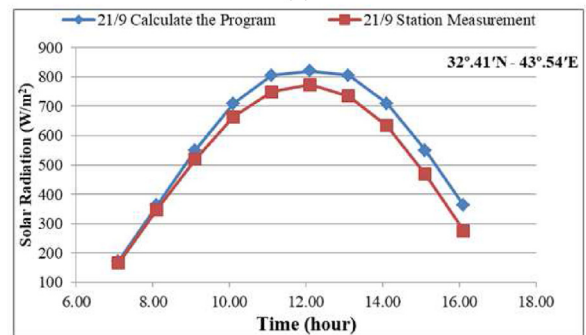
Fig. 2. Comparison between the measured and calculated data of solar radiation with time for site 2, in (a) 21/3, (b) 21/6, (c) 21/9, and (d) 21/12.



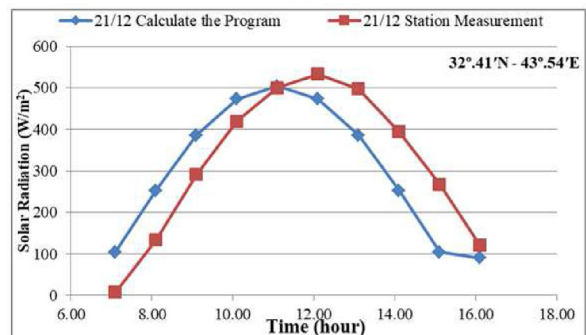
(a)



(b)



(c)



(d)

Fig. 3. Comparison between the measured and calculated data of solar radiation with time for site 3, in (a) 21/3, (b) 21/6, (c) 21/9, and (d) 21/12.

Fig. 3 shows the comparison between ground station data and space data for four times periods for site 3.

Curve's behavior is not the same all the time. There is a shift of the ground station curve in

Figures a, b, and d. As for Figure c, it appears that there is congruence between the two curves because of the difference in the angle of elevation of the sun this month, and the solar radiation sensor does not sense this difference at the top of the curves.

The behavior of the two curves in this site 3 is similar to the two curves in site 2. The shift towards the west means the same errors in the setting of the solar radiation sensor for the station.

This shift is less in the 9th month and increases in the other months due to the height or lowest of the solar elevation angle and its conformity with the level angle of the solar sensor.

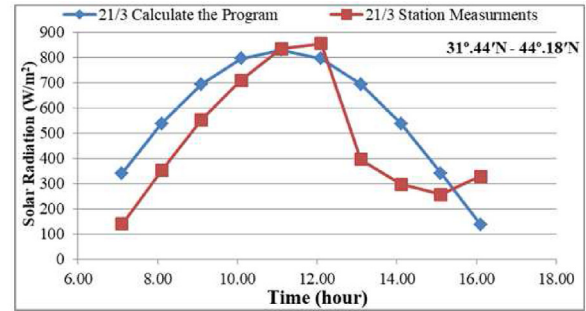
In Fig. 4, the comparisons for site 4 showed that the curves have the same behavior in hourly solar radiation rates from sunrise to sunset, the drop in ground weather station measurements due to the weather status, that there is an activity of clouds after midday of the site on this day in Fig. 4a and the agreement in behavior to hourly solar radiation from sunrise to sunset in Fig. 4b. But there is a shifting in the peak between the two curves due to attributed to the alignment of the station with the solar radiation sensor. Fig. 4c shows the two curves' same behavior to hourly solar radiation rates from sunrise to sunset. But in this case, the difference in the peak of the curves disappears. The reason could be the difference in the angle of elevation of the sun and its perpendicularity with the sensor. So, the sensitivity to the difference will be lower in the event that the sensor is not aligned with the station base. Fig. 4d shows the behavior of two curves in this site, the matching hourly solar radiation rates from sunrise to sunset. The difference in the peaks of the two curves disappears due to the decrease in the angle of elevation of the sun and perpendicular to the sensor, so the sensitivity to the difference between the peaks of the two curves is small.

In this site 4, the shift between the two curves is rare. There is a shift for the 3rd and 6th months and an agreement for the 9th and 12th months. This confirms that the alignment base station and the level solar sensor are incompatible.

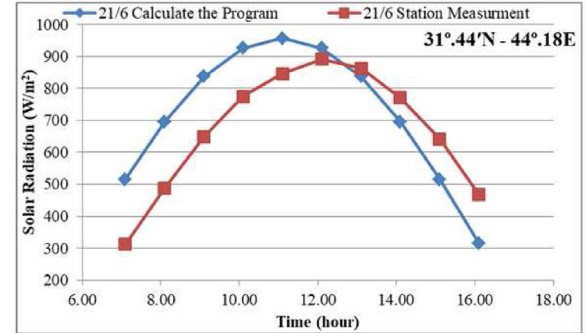
In Fig. 5, the comparison between ground station measurements and calculation of the program for site 5 showed the same behavior to hourly solar radiation from sunrise to sunset for all months. But the differences between the two curves for this site are less than for other sites, and the reason for the alignment of this station is more accurate.

In this site 5, it appears that in the two curves' behavior as the station curve, its outward behavior is more than that of the mathematical program curve, and this means that there is a difference in the field of view of the solar sensor from sunrise to sunset that differs from the field of vision of the other of the sensors sites.

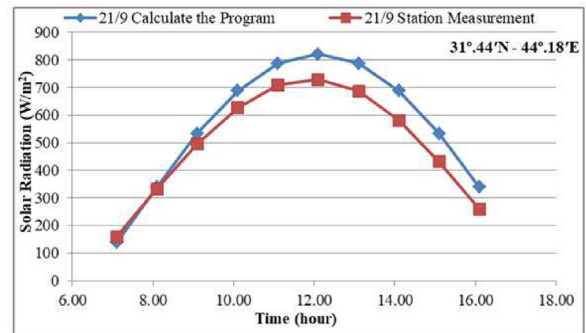
To observe the differences between the accuracy data between the Station Measurements (SM) and the closely Calculated Program (CP) data, Table 1.



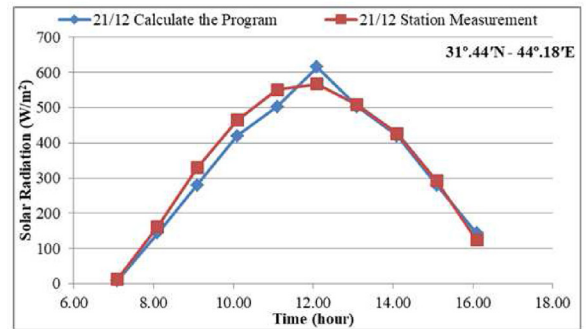
(a)



(b)



(c)



(d)

Fig. 4. Comparison between the measured and calculated data of solar radiation with time for site 4, in (a) 21/3, (b) 21/6, (c) 21/9, and (d) 21/12.

shows these differences on a 21/6 day. The data of the 21/6 day was selected for low radiation attenuation this month, which shows that one of the reasons for these differences is due to errors in the

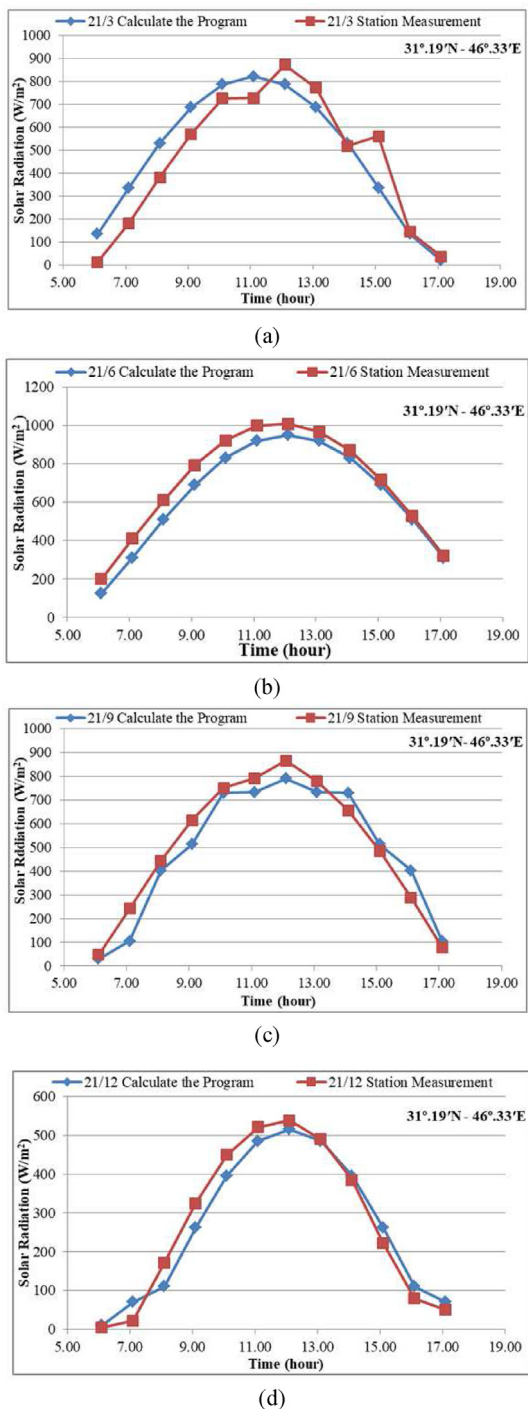


Fig. 5. Comparison between the measured and calculated data of solar radiation with time for site 5, in (a) 21/3, (b) 21/6, (c) 21/9, and (d) 21/12.

alignment of the station sensor, as well as the weather conditions surrounding the station.

It is necessary to combine data for the ground station with multiple sources of data in order to estimate solar radiation rates for high accuracy solar radiation. The following figures show the comparison between the PVGIS data and the data from five

ground stations used in this study to evaluate the data accuracy: from all figures seen rapprochement between two data, specialists in the sixth and ninth months for all sites. That is, the clarity of the atmosphere in these months and low attenuation in them; due to attenuation in these months and variations in diffuse solar radiation rates, there is little variation in solar radiation values in the third and twelfth months.

Fig. 6 shows the hourly solar radiation rates for the 3rd (a), 6th (b), 9th (c), and 12th (d) months for the site1 in the (32°19' E– 47°28'N) site. It is clear there is some difference between curves because the atmospheric attenuation for solar beam in this month from the clouds, humidity, and the diffuse beam is large in these times; the Figure shows a close between them on the clear days in this month.

Fig. 6a shows the ground station's solar radiation rates are the highest than the satellite solar radiation rates because the ground station rates data are real data, but the satellite data is processed, and the solar sensor is cleaner. Fig. 6b shows the great close of the two curves, and may the solar sensor be dusty, while the peak ground station data rates are lower than the satellite data rates this month due to the dustiness of the radiation sensor in Fig. 6c. Due to the cloud activity, Fig. 6d, the curve station data rates are lower than the satellite data rates.

We note from Fig. (6a–d) that the greater the quantities of processed data and for long periods completed for the month's data. The less the percentage of shifting between the data of the two curves and a massive difference between the two curves do not appear as it appears in the one-day data as it appears in the comparison between the two curves data of the ground station and the of the mathematical program data.

The differences that appear relatively between the ground station data and the satellite data are caused by the mathematical processing of the satellite data for long periods and considerable amounts of data, unlike the ground station data, which is realistic.

It is important to compare satellite data and ground station data to show the differences between them; Fig. 7a–d show the hourly solar radiation rates for the 3rd, 6th, 9th and 12th months in site 2. The curves have a close correlation.

The figures in site 2 show that the rates of solar radiation for the ground station for three months (3rd, 6th, 12th) are relatively higher than the rates of solar radiation for the satellite data, except for the 9th month it is lower, and the reason is as we know that in the summer months there is an amount of accumulated dust on the solar sensor, which attenuates the solar radiation beam reaching the solar

Table 1. Shows the differences between the Station Measurements (SM) and the Calculate Program (CP) data on 21/6.

Date 21/6								
Tilt Angle 0°								
Position	Sunrise SM (hour)	Sunrise CP (hour)	Sunset SM (hour)	Sunset CP (hour)	Peak SM		Peak CP	
					W/m ²	hour	W/m ²	hour
32°.19'N-47°.28'E	7.10	6.57	19.10	16.17	Cloudy	12.1	9484	12.1
31°.57'N-44°.46'E	7.10	6.55	16.10	16.16	889-3	12.1	952.1	11.1
32°.41'N-43°.54'E	7.10	6.57	16.10	16.17	955	13.1	945.5	11.1
31°.44'N-44°.18'E	7.10	6.55	16.10	16.17	8912	12.1	956.7	11.1
31°.19'N-46°.33'E	7.10	6.57	16.10	16.17	1007.1	12.1	945.3	12.1

sensor, and this also shows the same behavior in most other sites. However, the difference in the site of the ground station and the data of every month for each station and comparing it with the satellite data can give an indication of the accuracy of the data of the ground station and the possibility of its adoption in various solar energy applications. Fig. 8–d show the hourly solar radiation rates for the 3rd, 6th, 9th, and 12th months in site 3; it looks that the curves are coming to a close, and there are some diffuse beams and clarity for this site.

In some curves, it may be noted that there is a difference in the rates of solar radiation station at midday, and the reason may be due to the cleanliness of the sensor in this site and the absence of dust accumulation on it, as it recorded the highest rates of solar radiation, which appeared clearly different from the PV GIS data.

In site 3, a clear difference appears in the solar radiation rates between the two curves, especially at midday for the three months (3rd, 6th, 12th), except for the 9th month it is less due to the climate conditions for this site which differs from other sites and increasing of the amounts of dust. The behavior of the monthly curves is almost identical on all sites.

The solar radiation rates for site 4 are shown in Fig. 9, which illustrates the hourly solar radiation rates for the 3rd, 6th, 9th, and 12th months from sunrise to sunset. It is clear from these figures that it has the same curve patterns and some close correlation.

In some curves in Fig. 9, there may be a clear difference between the data, the reason is that the PVGIS data takes the data for a long period of time, so it is regular in its change with the days of the month, while the station data record data for a shorter period of time, so the fluctuation in the data is clearer.

It is noted in all curves that the same behavior for all sites in the two comparisons that there is an effect on the alignment of the ground station base with the solar sensor level, which determines the

solar sensor field of view, and thus its effect on the rates of solar radiation and determining midday, sunrise, and sunset.

Fig. 10 shows the hourly solar radiation rates for the 3rd, 6th, 9th, and 12th months in site 5. Due to the diffuse solar beam or the clarity and accuracy of PVGIS data on this site, there are some differences in curve behavior at midday.

Although site 5 is more suitable in two curves in both comparisons, it is also possible to notice a simple difference between the two curves in both comparisons for determining the amount of the solar radiation rate at midday because there is a difference in determining the peak in the middle of the day, for the same reasons for installing the ground station in all sites.

In order to clarify some of the differences closely between the accuracy data of the Station Measurements (SM) and the PV GIS data, Table 2 shows the data for the 6th month. It was selected for low radiation attenuation this month. There are some differences due to errors in the alignment of the station's sensor as well as the weather conditions surrounding the station.

The variations between the accuracy data of the Station Measurements (SM) and the PV GIS data vary from location to location, as shown in Table 2. This could be a result of the variable atmospheric conditions that affect the solar radiation in those regions.

It is clear from the area under the two curves in all sites in both comparisons lack of difference in the daily, monthly, and annual solar radiation rates if the ground station data is utilized in applications that do not require accuracy in determining the time of sunrise, sunset, and midday.

From the daily and monthly behavior of the data of the ground stations in all the sites, we can determine the most suitable site for solar energy applications, especially photovoltaic and thermal solar energy applications, in the face of climatic conditions and the amounts of increasing dust.

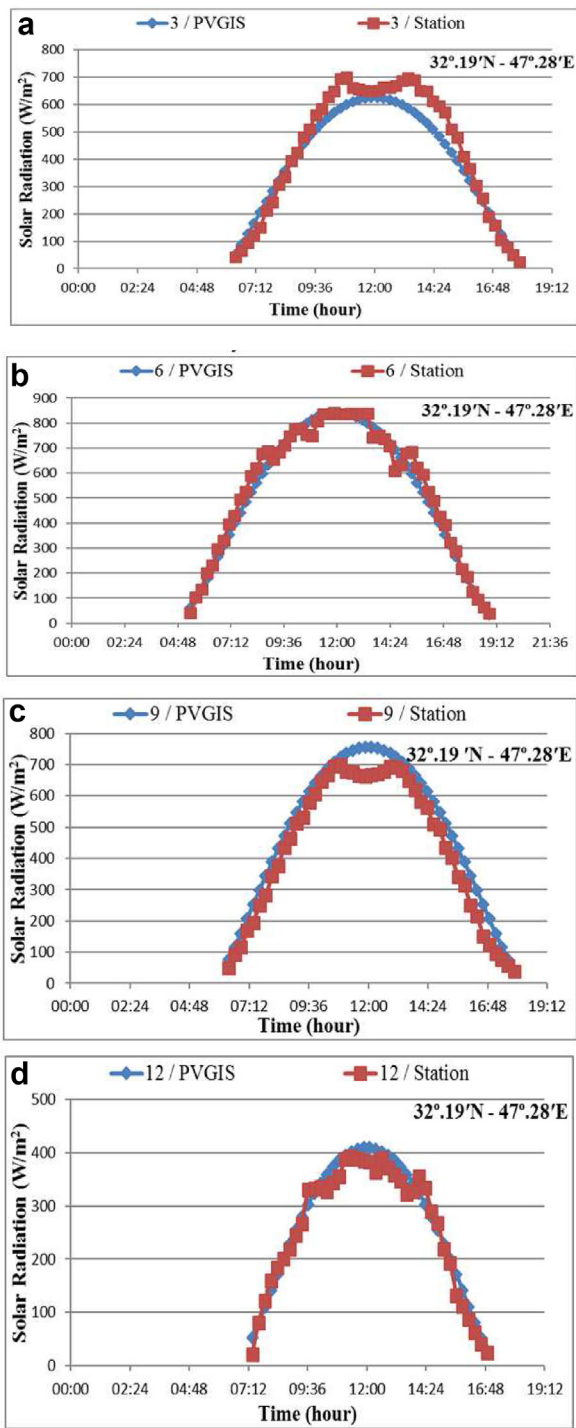


Fig. 6. a. The fluctuation of the solar radiation rate of the ground station data compared to the PVGIS data for site 1 in the 3rd month. b. Fluctuation and some match in the ground station data relative to the PVGIS data for site 1 in the 6th month. c. Some match solar radiation rates for the ground station data compared to the PVGIS data for site 1 in the 9th month. d. The fluctuation of the solar radiation rate of the ground station data compared to the PVGIS data for site 1 in the 12th month.

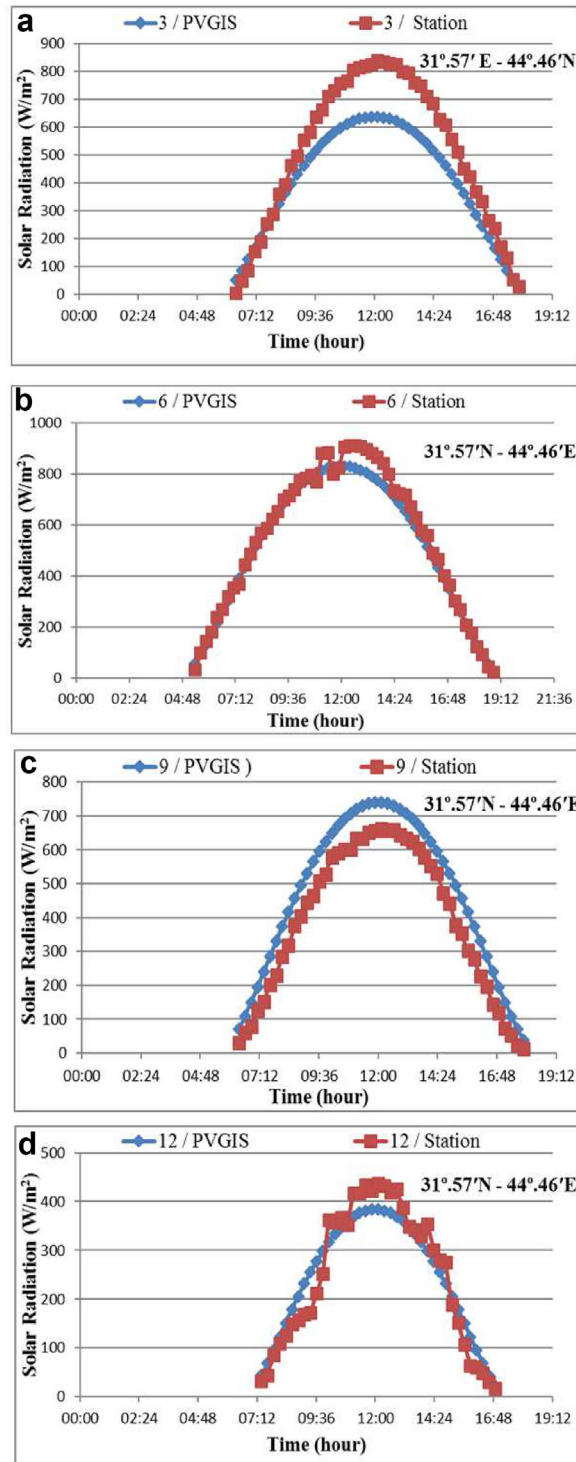


Fig. 7. a. High solar radiation rates in the middle of the day for the ground station data compared to the PVGIS data for site 2 in the 3rd month. b. Relative match between ground station data and PVGIS data for site 2 in the 6th month. c. Close of in the behavior between ground station data with PVGIS data for site 2 in the 9th month. d. A clear fluctuation of the ground station data compared to the PVGIS data for site 2 in the 12th month.

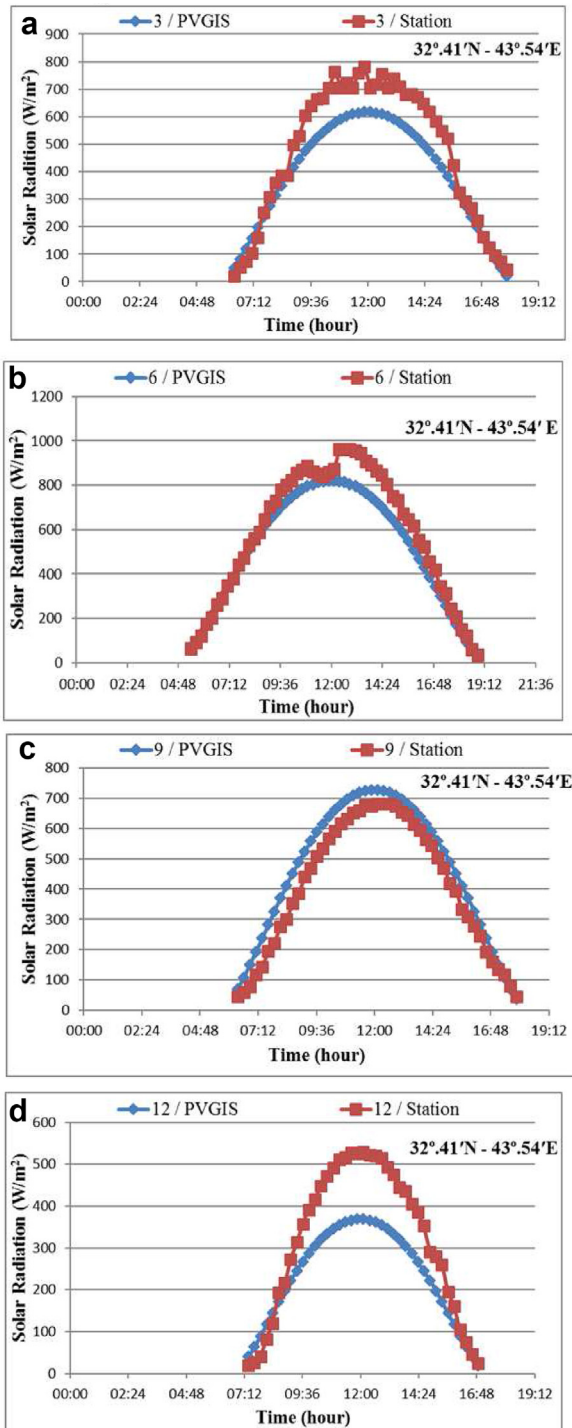


Fig. 8. a. Height and fluctuation in the data of the solar radiation rates of the ground station compared to the data of the PVGIS for site 3 in the 3rd month. b. There is a match between the behavior of the ground station data with the PVGIS data at sunrise and sunset with a change in the middle of the day for site 3 in the 6th month. c. There is a matching between ground station data and PVGIS data for site 3 in the 9th month. d. An increase in the solar radiation rates data for the ground station in the middle of the day compared to the PVGIS data for site 3 in the 12th month.

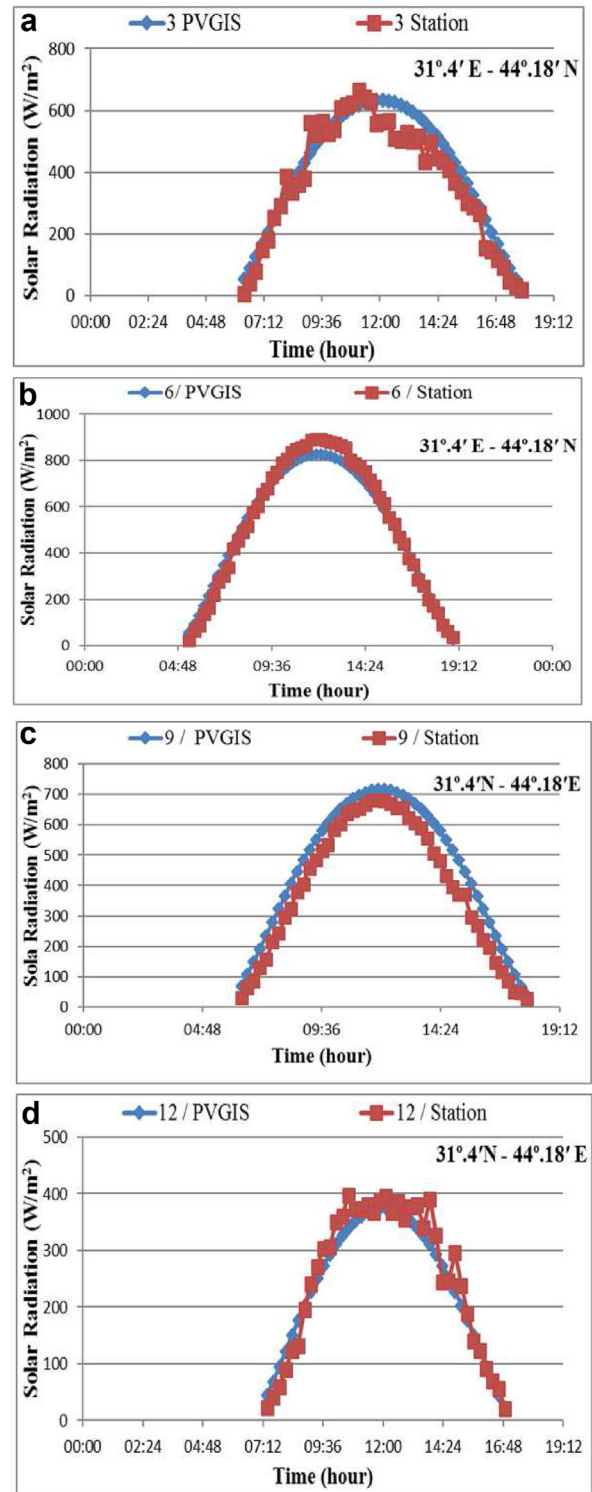


Fig. 9. a. There is fluctuation in the data of the solar radiation rates of the ground station compared to the PVGIS data for site 4 in the 3rd month. b. The matching between ground station data and PVGIS data for site 4 in the 6th month. c. The matching between ground station data and PVGIS data for site 4 in the 9th month. d. There is fluctuation in the data of the solar radiation rates of the ground station compared to the PVGIS data for site 4 in the 12th month.

4. Conclusions

Accurate and reliable solar radiation data is necessary to compare the solar radiation data coming in from different sources to determine their level of accuracy. It can conclude that a simple correlation between the data of the ground station and the program and the PV GIS data, the reason for the difference between the accuracy of the data for these sources is related to technical reasons for the ground station. The accuracy of this data can be relatively adopted in the estimation process in multiple applications for some stations, including solar energy applications, if the data is processed to overcome errors. For reliable measurement results, the quality of the installed measuring devices must be carefully considered, as in the classification of pyranometers. These ground stations need regular maintenance, cleaning, alignment, and docking of the solar sensors to obtain accurate data. The three data sources can be combined to improve the accuracy of station data.

References

- [1] J. Ren, eds., *Renewable-Energy-Driven Future*, Elsevier Science Publishing Co Inc, San Diego. (2020).
- [2] E.O. Ogundimu, E.T. Akinlabi, C.A. Mgbemene, Maximizing the output power harvest of A pv panel: a critical review, *J Phys Conf Ser* 1378 (2019) 032054, <https://doi.org/10.1088/1742-6596/1378/3/032054>.
- [3] M.A.M. Ramli, S. Twaha, K. Ishaque, Y.A. Al-Turki, A review on maximum power point tracking for photovoltaic systems with and without shading conditions, *Renew Sustain Energy Rev* 67 (2017) 144–159, <https://doi.org/10.1016/j.rser.2016.09.013>.
- [4] A.H.A. Al-Waeli, H.A. Kazem, M.T. Chaichan, K. Sopian, *The impact of climatic conditions on PV/PVT outcomes, photovoltaic/thermal syst*, Springer. (2019), https://doi.org/10.1007/978-3-030-27824-3_5.
- [5] I.S. Panagea, I.K. Tsanis, A.G. Koutroulis, M.G. Grillakis, Climate change impact on photovoltaic energy output: the case of Greece, *Adv Meteorol* 2014 (2014) 264506, <https://doi.org/10.1155/2014/264506>.
- [6] F.J. Diez, A. Martínez-Rodríguez, L.M. Navas-Gracia, L. Chico-Santamarta, A. Correa-Guimaraes, R. Andara, Estimation of the hourly global solar irradiation on the tilted and oriented plane of photovoltaic solar panels applied to greenhouse production, *Agronomy* 11 (2021) 495, <https://doi.org/10.3390/agronomy11030495>.
- [7] T. Mishra, A. Rabha, U. Kumar, K. Arunachalam, V. Sridhar, Assessment of solar power potential in a hill state of India using remote sensing and Geographic Information System, *Remote Sens Appl Soc Environ* 19 (2020) 100370, <https://doi.org/10.1016/j.rsase.2020.100370>.
- [8] K.V. Vidyandandan, An overview of factors affecting the performance of solar PV systems, *Energy Scan* 27 (2017) 2–8.
- [9] J. Walters, J. Kaminsky, L. Gottschamer, A systems analysis of factors influencing household solar PV adoption in Santiago, Chile, *Sustain Times* 10 (2018) 1257, <https://doi.org/10.3390/SU10041257>.
- [10] J. Möllenkamp, T. Beikircher, A. Häberle, Recalibration of SPN1 pyranometers against pyrhemliometer and its relevance for the evaluation of concentrating solar process heat plants, *Sol Energy* 197 (2020) 344–358, <https://doi.org/10.1016/j.solener.2019.12.055>.
- [11] J.L. Balenzategui, F. Fabero, J.P. Silva, Solar radiation measurement and solar radiometers, *Green Energy Technol*, Springer. (2019), https://doi.org/10.1007/978-3-319-97484-2_2.
- [12] K. Lovegrove, W. Stein, *Concentrating solar power technology: principles, developments and applications*, Woodhead Publishing Limited. (2012), pp. 1–674, <https://doi.org/10.1533/9780857096173>.
- [13] T. Betti, I. Zulim, S. Brkić, B. Tuka, A comparison of models for estimating solar radiation from sunshine duration in Croatia, *Int J Photoenergy* 2020 (2020) 9605950, <https://doi.org/10.1155/2020/9605950>.
- [14] A.A. Jadallah, D.Y. Mahmood, Z.A. Abdulqader, Estimation and simulation of solar radiation in certain Iraqi Governorates, *Int J Sci Res* 3 (2012) 945–949.
- [15] G. Salima, G.M.S. Chavula, G. Salima, G.M.S. Chavula, Determining angstrom constants for estimating solar radiation in Malawi, *Int J Geosci* 3 (2012) 391–397, <https://doi.org/10.4236/IJG.2012.32043>.
- [16] N.W.S, US Department of commerce, NOAA, National weather Service. <https://www.weather.gov/>. (accessed September 27 2021).
- [17] A. Meque, S. Gamedze, T. Moitlhobogi, P. Booneeady, S. Samuel, L. Mpalang, Numerical weather prediction and climate modelling: challenges and opportunities for improving climate services delivery in Southern Africa, *Clim Serv* 23 (2021) 100243, <https://doi.org/10.1016/j.cliser.2021.100243>.
- [18] D.R. Arumugham, P. Rajendran, Modelling global solar irradiance for any location on earth through regression analysis using high-resolution data, *Renew Energy* 180 (2021) 1114–1123, <https://doi.org/10.1016/j.renene.2021.09.030>.
- [19] I. García, M. de Blas, B. Hernández, C. Sáenz, J.L. Torres, Diffuse irradiance on tilted planes in urban environments: evaluation of models modified with sky and circumsolar view factors, *Renew Energy* 180 (2021) 1194–1209, <https://doi.org/10.1016/j.renene.2021.08.042>.
- [20] J. Qiu, X. Zong, J. Yang, X. Xia, Season-dependent uncertainties in baseline surface radiation network (BSRN) solar radiation data, *Atmos Res* 248 (2021) 105240, <https://doi.org/10.1016/j.atmosres.2020.105240>.
- [21] A. Rouholamini, H. Pourgharibshahi, R. Fadaeinedjad, M. Abdolzadeh, Temperature of a photovoltaic module under the influence of different environmental conditions – experimental investigation, *Int J Ambient Energy* 37 (2016) 266–272, <https://doi.org/10.1080/01430750.2014.952842>.
- [22] A.B. Jenkin, J.P. McVey, M.E. Sorge, Assessment of time spent in the LEO, GEO, and semi-synchronous zones by spacecraft on long-term reentering disposal orbits, in: *Proc. Int. Astronaut. Congr. IAC*, 2020.
- [23] Y.M. Govaerts, F. Rüthrich, V.O. John, R. Quast, Climate data records from Meteosat first generation part I: simulation of accurate top-of-atmosphere spectral radiance over pseudo-invariant calibration sites for the retrieval of the in-flight visible spectral response, *Remote Sens* 10 (2018) 1959, <https://doi.org/10.3390/rs10121959>.
- [24] A. Higuchi, Toward more integrated utilizations of geostationary satellite data for disaster management and risk mitigation, *Remote Sens* 13 (2021) 1553, <https://doi.org/10.3390/rs13081553>.
- [25] H. Letu, K. Yang, T.Y. Nakajima, H. Ishimoto, T.M. Nagao, J. Riedi, A.J. Baran, R. Ma, T. Wang, H. Shang, C. Shi, J. Shi, High-resolution retrieval of cloud microphysical properties and surface solar radiation using Himawari-8/AHI next-generation geostationary satellite, *Remote Sens Environ* 239 (2020) 111583, <https://doi.org/10.1016/j.rse.2019.111583>.
- [26] J. Chen, W. Zhu, Q. Yu, Estimating half-hourly solar radiation over the Continental United States using GOES-16 data

- with iterative random forest, *Renew Energy* 178 (2021) 916–929, <https://doi.org/10.1016/j.renene.2021.06.129>.
- [27] C. Vernay, S. Pitaval, P. Blanc, Review of satellite-based surface solar irradiation databases for the engineering, the financing and the operating of photovoltaic systems, *Energy Proc* 57 (2014) 1383–1391, <https://doi.org/10.1016/j.egypro.2014.10.129>.
- [28] S. Hosseinzadeh, K. Hosseinzadeh, A. Hasibi, D.D. Ganji, Thermal analysis of moving porous fin wetted by hybrid nanofluid with trapezoidal, concave parabolic and convex cross sections, *Case Stud Therm Eng* 30 (2022) 101757, <https://doi.org/10.1016/j.csite.2022.101757>.